Hydrol. Earth Syst. Sci. Discuss., 6, 2537–2571, 2009
www.hydrol-earth-syst-sci-discuss.net/6/2537/2009/

Hydrology and Earth System Sciences Discussions

Papers published in *Hydrology and Earth System Sciences Discussions* are under open-access review for the journal *Hydrology and Earth System Sciences*

Reducing the hydrological connectivity of gully systems through vegetation restoration: combined field experiment and numerical modelling approach

A. Molina[1], **G. Govers**[1], **A. Van den Putte**[1], **and V. Vanacker**[2]

[1]Physical and Regional Geography Research Group, Katholieke Universiteit Leuven, Celestijnenlaan 200E, 3001 Heverlee, Belgium
[2]Department of Geography, University of Louvain, 3 Place Louis Pasteur, 1348 Louvain-la-Neuve, Belgium

Received: 7 March 2009 – Accepted: 12 March 2009 – Published: 23 March 2009

Correspondence to: A. Molina (armando.molinaverdugo@ees.kuleuven.be)

Published by Copernicus Publications on behalf of the European Geosciences Union.

Abstract

Restoration of degraded land in the southern Ecuadorian Andes has led to alterations in the functioning of degraded catchments. Recovery of vegetation on areas affected by overgrazing, as well as the reforestation or afforestation of gully areas have given rise to modifications of hydrological connectivity within the catchments. Recent research has highlighted the ability of gully channels to trap sediment eroded from steep slopes, especially if vegetation is established along the gully bed. However, vegetation cover not only induces sediment deposition in the gully bed, but may also have a potential to reduce runoff water volume. The performance of gully beds in reducing the transfer of runoff water was investigated by conducting controlled concentrated flow experiments in the field. Experimental field data for 9 gullies were derived by pouring concentrated inflow into the upstream end of the gully channel and measuring the outflow at the downstream end of the channel. Two consecutive flow experiments per gully were carried out, so that data for dry and wet soil conditions were collected. The hydrological response to concentrated flow was estimated for each experiment by calculating its cumulative infiltration coefficient, IC (%). The results showed a great difference in IC between dry and wet soil conditions. The IC for wet soil conditions was on average 24%, whereas it was 60% for dry conditions. Gullies with more than 50% surface vegetation cover exhibit the highest cumulative infiltration coefficients (81% for “dry runs”, and 34% for “wet runs”), but runoff transmission losses were not as clearly related to vegetation cover as sediment storage. The experimental field data of 16 experiments were used to calibrate a hydrological model in order to simulate the transfer of concentrated flow along the gully beds. The model is based on (i) the Philip’s equation to simulate runoff water infiltration and (ii) the kinematic wave approximation to simulate runoff routing. The model is able to predict the transfer of runoff water generally well, as the error on the predicted total outflow volumes is below 13% for 15 out of 16 cases. The sensitivity analysis indicates that the most sensitivity parameters to predictions of transfer of runoff flow in the gully channel are sorptivity S, hydraulic conductivity K and

runoff width W. The high sensitivity of model results to some crucial hydraulic parameters is one of the reasons why the relationships between model parameter values and gully features are relatively weak.

The results obtained from the field experiments and the kinematic wave model show that gully systems are key elements in the hydrological connectivity of degraded landscapes. The transfer of overland flow and sediment from the slopes towards the river system highly depends on the presence/absence of vegetation in the gully beds and should therefore be accounted for in assessments of landscape degradation and/or recovery.

1 Introduction

Mountain ecosystems fulfill essential hydrological functions, as they are the source of water for more than half of the global population. Their hydrological functioning is often complex, as rainfall-runoff processes are both spatially and temporally highly variable and dependent on topography, vegetation type and cover, lithology, soil and rainfall characteristics (Seibert and MacGlynn, 2005). In natural conditions, humid mountain environments with steep slopes and active slope processes tend to have thin sandy to stony soils and relatively good infiltration rates (Janeau et al., 2003). Land use strongly alters the hydrological functioning of mountain catchments (e.g. Ziegler et al., 2007). Rainfall simulation experiments in heavily disturbed mountainous catchments have demonstrated that the disturbance of natural vegetation changes runoff generation mechanisms (Harden, 1991, 2006; Molina et al., 2007). Soil compaction and truncation following agricultural activities are shown to induce Hortonian overland flow, a phenomenon rarely observed in natural mountain forests (Bruijnzeel, 2004; Molina et al., 2007).

The generation of Hortonian overland flow can lead to the development of extensive badlands and gullies on overgrazed and/or abandoned agricultural land. The Hortonian overland flow produced on bare badland slopes is likely to disrupt significantly the

HESSD
6, 2537–2571, 2009

Reducing the hydrological connectivity of gully systems

A. Molina et al.

natural hydrological regime, as badlands not only generate large volumes of water and sediment, but also transport them efficiently to the river network. The dense network of rills and gullies directly connected to tributaries and main river channels plays a key role in connecting sources of water and sediment with the river system (Croke et al., 2005). Any change in the state of the gully network may affect the hydrological connectivity by modifying the transfer of water and sediment from slopes to the river network, and hence influence the hydrological response of the catchment (Bracken and Croke, 2007).

Results from experimental sites have shown that revegetation of the gully bed alters its geomorphological response, and can even make gullies evolve from sediment sources to sediment sinks. Sediment trapping by vegetation in the gully bed was observed for marly gullies with only partial vegetation cover (33%) in the French Southern Alps (Rey, 2003), for gullies incised in loess (Nachtergaele et al., 2002) as well as for steep afforested gullies in the Ecuadorian Andes (Molina et al., 2009). Several mechanisms co-operate to favour sediment trapping in vegetated gully beds: vegetation generally increases flow resistance, reduces runoff water velocity and sediment transport capacity, thereby inducing sediment deposition (Temple, 1982, 1983; Tsujimoto, 1999; López and García, 2001). The vegetation cover prevents the sediment from being eroded, and its root system anchors the deposited material (Prosser et al., 1995; Rey, 2004). The establishment of grassed waterways in arable land builds on these principles to reduce sediment production (Fiener and Auerswald, 2003).

Gully bed stabilisation most likely not only affects sediment but also water storage and transmission. However, in spite of the field knowledge gained on gully stabilization following gully bed revegetation (Nachtergaele et al., 2002; Rey, 2003; Molina et al., 2009), quantitative measures of the effect of the above-described modifications in gully conditions on the hydrological and sediment connectivity of restored catchments are rare. In this study, we focus on the role of vegetation in modifying the hydrological connectivity of restored gully systems. We particularly analysed the performance of gully channels to transfer flow of runoff water, in relation to the vegetation state of the gully channel. Nine ephemeral gullies were selected representing a wide range in gully bed vegetation cover. Large controlled concentrated flow experiments were completed in the field. We supplied a constant inflow to the upstream end of the gully channel, and measured flow depth, flow width and water front advance at several sections along the channel and the outflow at the downstream end of the gully channel. The experimental data were used to calibrate a hydrological model that allows us to simulate the transfer of concentrated flow along gully beds with different vegetation cover while accounting for runoff water infiltration. Our modelling approach is based on the concepts developed by Muñoz-Carpena et al. (1993, 1999) and Deletic (2001) for vegetative filter strips and Fiener and Auerswald (2005) for grassed waterways. The model uses the kinematice wave for routing runoff flow, and the Philip's equation for simulating runoff water infiltration.

2 Materials and methods

2.1 Study area

Nine ephemeral gullies in the Jadan catchment (southern Ecuadorian Andes) were selected to represent a wide range in vegetation cover of the gully bed. The Jadan catchment is representative for highly degraded Andean ecosystems. The catchment ranges in elevation from 2290 to 3330 m a.s.l. and has a surface area of 296 km^2. The region is characterized by a tropical mountain climate (Dercon et al., 1998), and mean annual rainfall measured at the station of Cochapamba-Quingeo is about 810 mm, but it is known be significantly higher at higher altitudes. The landscape is highly dissected, and dominated by moderate to steep soil-mantled hill slopes. The lower section of the Jadan river valley has gentle slopes, and several levels of alluvial terraces are present. The major part of the catchment area comprises late-Miocene to Pliocene volcanoclastic and sedimentary rocks (Hungerbühler et al., 2002).

Land use in the Jadan catchment is dynamic, and responds quickly to changing socio-economic and demographic settings (White and Maldonado, 1991; Vanacker et al., 2003). Native forest has been transformed into a mosaic of anthropogenic land uses. Some remnants of native forest are today only present at remote locations at high altitude. Cleared land is used for intensive crop farming and animal grazing. The reduction of the protective vegetation cover and deterioration of the soil chemical and physical properties has accelerated the development of deep gully systems on loosely consolidated and deeply weathered volcanoclastic and sedimentary rocks, especially on the grazing lands (Vanacker et al., 2007). Declining soil fertility, soil compaction and rill and gully erosion resulted in increasing land abandonment and vegetation restoration (Harden, 1996; Vanacker et al., 2003). The vegetation cover of the lower and middle part of the catchment is now slowly increasing through natural revegetation following abandonment and afforestation of degraded land (Molina et al., 2007).

2.2 Characterization of the gullies and field measurements

Before running the concentrated flow experiments, we characterized the state of the gully bed for all ephemeral gullies. The upstream area of the gullies varies from 287 to 934 m^2, the length of the gully bed ranges from 39 to 59 m, and the average gully bed width ranges from 0.41 to 1.78 m. Each gully was divided into 5-m length segments. The ground and canopy vegetation cover, the volume of sediment accumulation, and slope gradient were measured for each segment. A total number of 80 gully segments were characterized for this study. The ground vegetation cover of each segment was determined as the percentage of the surface area of the gully bed that is covered by a combination of woody vegetation (*Alnus jorullensis, Eucalyptus globulus*, and *Pinus radiate*), shrubs (*Cortaderia rudiuscula, Spartium junceum* and *Baccharis polyantha*), and grassy plants (*Pennisetum clandestinum, Holcus lanatus, Festuca megalura* and *Cynodon dactylon*). We refer to Molina et al. (2009) for more detailed information. Before and after the flow experiments, core samples of the gully bed material were taken using small steel cylinders to determine the grain size distribution of the gully bed material, its moisture content and bulk density.

Flow discharge was released from a 9850 litres (2600 US gallons) tank truck, and then transferred to a 1 m^3 container through a hose connection. The water level in the latter container was kept as steady as possible using a control valve so that the discharge supplied to the upstream end of the gully channel was as constant as possible (Fig. 1). At the gully outlet an H-flume was installed in order to measure outflowing discharge. From the start of the concentrated flow measurements, we monitored the advance of the water front. Based on the distance travelled during a certain time interval, we calculated the rate of advance of the water front. At regular time intervals, we also measured flow depth and width at several locations along the gully bed. The mean flow velocity, V ($\mathrm{m\,s^{-1}}$), was estimated using Manning's formula:

$$V = \frac{R^{2/3} S^{1/2}}{n} \tag{1}$$

Where n is the Manning's roughness coefficient, R is the hydraulic radius (m), and S is the slope of energy grade line approximated by the slope gradient of the gully bed ($\mathrm{m\,m^{-1}}$). The Manning's resistance coefficient for vegetation was estimated following the procedure for additive resistance developed by Cowan (1956):

$$n = (n_0 + n_1 + n_2 + n_3 + n_4)m \tag{2}$$

where n_0 is the base value for a straight, uniform, smooth channel in natural materials, n_1 is an additive value to account for surface irregularities, n_2 is added to account for variations in the channel geometry along the reach, n_3 is an additive value to account for obstructions, n_4 accounts for vegetation, and m is a correction factor for meandering or sinuosity of the channel. The n_4 coefficient used in Cowan's method is based on the net effect of vegetation. Based on our estimated mean flow velocity, we derived the Froude number F :

$$F = \frac{V}{\sqrt{gd}} \tag{3}$$

Where g is the acceleration due to gravity ($\mathrm{m\,s^{-2}}$) and d is the flow depth (m).

Large controlled concentrated flow experiments were completed for nine ephemeral gullies with different vegetation cover. Two consecutive flow experiments were carried out per gully, in order to collect data for dry and wet soil conditions. Each experimental run lasted between 20 and 55 mins. For the wet runs, this was sufficient to reach a steady-state discharge at the gully outlet.

2.3 Model description

The model that is developed for simulating routing of concentrated flow in gully beds is conceptually similar to the model developed by Fiener and Auerswald (2005) for grassed waterways on agricultural land. For a detailed description of the model we refer to Fiener and Auerswald (2005). Figure 2 is a schematic illustration of our model framework. We divided each gully into n segments of length Δx. Runoff water, here denoted as inflow q_{in}, is delivered to the first gully segment. A fraction of the total inflow infiltrates in the gully bed. When the soil infiltration capacity of the gully bed is exceeded, small micro-depressions start to fill by surface retention. Only when the storage capacity of the first gully segment is full, water starts to flow to the second gully segment. As infiltration continues in the first gully segment, the inflow q_{in} delivered to the second segment is reduced. The model describes the three above-described processes simultaneously: i.e. (i) surface infiltration, (ii) filling of surface storage and (iii) surface runoff.

2.3.1 Infiltration

Infiltration in the gully bed depends on the bed material, and its moisture content. To simplify the hydrological model, we assume that vertical infiltration is the dominant infiltration process, and that horizontal infiltration is negligible. Fiener and Auerswald (2005) adopted the Philip's equation (Eq. 4) for the infiltration component of the model, which is a mathematical solution of the Richard's equation applied to vertical infiltration (Philip, 1969; Hillel, 1998):

$$i(t) = \frac{1}{2 \cdot \sqrt{t}} \cdot S + K \tag{4}$$

where $i(t)$ is the infiltration rate ($\mathrm{m\,s^{-1}}$), t is the time (s), S is the sorptivity ($\mathrm{m\,s^{-0.5}}$), and K is the hydraulic conductivity ($\mathrm{m\,s^{-1}}$).

2.3.2 Surface retention

Surface retention is the amount of water that is stored above ground in small micro-depressions. This storage volume depends on the roughness of the gully bed, its vegetative cover and slope. Deletic (2001) showed that surface retention in grassed areas can be substantial, and often equal in magnitude to the total depth of a small to medium rainfall event. Here, we follow the approach of Fiener and Auerswald (2005) developed for grassed waterways, and estimated the surface retention volume as the product of the measured average flow depth and the wetted surface area.

2.3.3 Surface runoff

Unsteady flow in open channels is commonly described by one-dimensional Saint-Venant equations (1881) and based on the equations of continuity (Eq. 5) and momentum (Eq. 6) (Chow et al., 1988):

$$\frac{\partial Q}{\partial x} + \frac{\partial A}{\partial t} = q \tag{5}$$

$$\frac{\partial V}{\partial t} + V \cdot \frac{\partial V}{\partial x} + g \cdot \frac{\partial y}{\partial x} = g \cdot (S_0 - S_f) \tag{6}$$

where $Q(x,t)$ is the discharge ($\mathrm{m^3\,s^{-1}}$), $A(x,t)$ is the cross-sectional area of the flow ($\mathrm{m^2}$), x is the distance in flow direction (m), t is the time (s), q is the lateral inflow ($\mathrm{m^2\,s^{-1}}$), V is the average flow velocity ($\mathrm{m\,s^{-1}}$), g is the gravitational acceleration

($m\,s^{-2}$), y is the flow depth (m), S_0 is the dimensionless bed slope and S_f is the dimensionless friction slope.

In this work, we used kinematic flow approximations to simulate the flow of runoff water in gully channels. Kinematic flow routing is a simplification of the Saint-Venant equations of one-dimensional flow (Lighthill and Woolhiser, 1955), and assumes that the flow remains one-dimensional and uniform along the channel, and that channel boundaries are fixed (i.e. non-eroding or non-aggrading, Woolhiser, 1975). In kinematic flow conditions, the weight component of the flow (gravity force) is approximately balanced by the flow resistance (friction force) due to channel bed friction. A kinematic wave appears as uniform unsteady flow in the channel bed, and water and channel bed surfaces are considered to be parallel to each other and to the energy grade line. This routing scheme was already successfully applied for modelling surface runoff in grassed waterways (Fiener and Auerswald, 2005) and vegetated filter strips (Muñoz-Carpena et al., 1993, 1999; Delectic, 2001). As we are working here in steep gully channels with no back water effect, kinematic flow approximations are particularly suitable.

By applying a kinematic wave approach, the momentum Eq. (6) is replaced by a unique relation between the mean velocity and the flow depth. By doing so, only the gravity and friction slope terms are retained, and the momentum equation is reduced to $S_0=S_f$. The relation between Q and A in the continuity Eq. (5) can then be expressed by the Manning's Eq. (7).

$$Q = \frac{1}{n} \cdot \sqrt{S} \cdot R^{\frac{2}{3}} \cdot A \tag{7}$$

where Q is the discharge ($m^3\,s^{-1}$), n is the Manning's roughness coefficient ($m\,s^{-1/3}$) dependent on soil surface condition and vegetative cover, S is the dimensionless slope of the channel floor, R is the hydraulic radius (m) and A is the cross-sectional area of flow (m^2). We replaced the hydraulic radius, R, by A/w, with A the cross-sectional area and w the hydraulic perimeter (m). The Manning's equation can then be written as

$$A = \left[\frac{n \cdot w^{\frac{2}{3}}}{\sqrt{S}}\right]^{\frac{3}{5}} \cdot Q^{\frac{3}{5}} \tag{8}$$

Assume now $\alpha = \left[\frac{n \cdot w^{\frac{2}{3}}}{\sqrt{S}}\right]^{\frac{3}{5}}$ and $\beta = \frac{3}{5}$, then. $A = \alpha \cdot Q^{\beta}$

The continuity equation can then be written in function of a single dependent variable (Chow et al., 1988).

$$\frac{\partial Q}{\partial x} + \alpha\beta Q^{\beta-1}\frac{\partial Q}{\partial t} = q \tag{9}$$

This simplified form of the kinematic wave Eq. (9) describes the distribution of flow as function of the distance x along the channel bed and the time t.

We solved the kinematic wave equation numerically using an explicit finite difference approach. Figure 3 illustrates the outline of the computational grid that we used for discretization of the continuity equation. It divides the distance-time (x, t) space into intervals of a fixed distance (Δx) and time (Δt). A network of discrete points is thus obtained, and the flow variable, Q, is then derived only for this finite number of grid points. Our approximation uses the initial input parameters of α, β, and q (lateral inflow), and estimates the partial derivatives, $(\delta Q/\delta x)$ and $(\delta Q/\delta t)$, using a forward difference approximation. The value of Q in the term $\alpha\beta Q^{\beta-1}$ was estimated as an average of the $Q(x, t)$ values along the diagonal (Fig. 3). Hence, the following formula is obtained for predicting Q_{i+1}^{j+1}.

$$Q_{i+1}^{j+1} = \frac{\frac{\Delta t}{\Delta x} Q_i^{j+1} + \alpha\beta Q_{i+1}^{j}\left(\frac{Q_i^{j+1} + Q_{i+1}^{j}}{2}\right)^{\beta-1} + q\Delta t}{\frac{\Delta t}{\Delta x} + \alpha\beta\left(\frac{Q_i^{j+1} + Q_{i+1}^{j}}{2}\right)^{\beta-1}} \tag{10}$$

HESSD

6, 2537–2571, 2009

Reducing the hydrological connectivity of gully systems

A. Molina et al.

where $\alpha = \left[\frac{n \cdot w^{\frac{2}{3}}}{\sqrt{S}}\right]^{\frac{3}{5}}$, and $\beta = 3/5$.

It is known that solving the continuous kinematic wave equation by finite differences can introduce numerical errors into the results. These errors can be amplified with successive calculations of grid points along a time line. Here, we avoided numerical instability by taking small values of Δx (5 m) and Δt (5 s). This resulted in a Courant number always well below 1.

2.3.4 Parametrization

The input parameters for the kinematic wave model are listed in Table 1. Various parameters were directly measured in the field during the flow experiments, such as the inflow rates at the upstream end of the gully channel, the flow depth and flow width at several locations along the gully bed and the slope of the gully bed. The Manning's roughness coefficient, n, was estimated by the Cowan method (Eq. 2). The lateral inflow rate, q, is computed as the difference between the rainfall rate and the infiltration rate in the channel bed. As the experiments were carried out in dry weather conditions, the lateral inflow rate equals the infiltration rate. The time-dependent infiltration function, here described by the Philip's Eq. (4), was solved for each grid point of the computational grid. The values of sorptivity, S, and hydraulic conductivity, K, were calibrated to observed outflow hydrographs. As the lateral flow parameter of the kinematic wave model (q) is expressed in $m^3\,m^{-1}\,s^{-1}$ (i.e. the lateral flow per gully bed length per time unit), the values obtained by the Philip's equation (i.e. infiltration rate per surface area per time unit, $m^3\,m^{-2}\,s^{-1}$), are multiplied with the corresponding gully bed width.

3 Analysis and discussion of experimental data

3.1 Role of vegetation on infiltration and runoff transfer

We completed 18 concentrated flow experiments, one experiment under dry and wet conditions for each gully: 17 out of 18 experiments experienced outflow at the downstream end of the gully channel. For the Quingeo gully, the amount of water supplied in the dry run was unable to produce any outflow. Furthermore, we noticed that the transmission of runoff was spatially very heteregeneous in this gully, with a rapid water transfer in the upper part and a very slow tranmission in the lower, heavily vegetated part. We therefore did not take the results from this gully into account in the further analysis as we considered the spatial heterogeneity within the gully too big for it to be considered as a single system. Thus, 16 observations were retained for further analysis.

The total inflow, RI (m^3), varied from 1.67 to 5.99 m^3, with an average value of 2.93 m^3±1.19, and the total outflow, RO (m^3), varied from 0.19 to 3.54 m^3, with an average value of 1.49 m^3±0.76 (Table 2). The hydrological response to concentrated flow was estimated for each experiment by calculating the cumulative infiltration coefficient, IC (%) :

$$IC = \left[(RI - RO)/RI\right] \times 100 \tag{11}$$

Clear differences in cumulative infiltration were observed for experiments under dry and wet hydrological conditions (Table 2). Cumulative infiltration coefficients measured under dry conditions varied between 34 and 100%, with an average value of 60%±23; whereas the coefficients under wet conditions ranged between 1 and 70%, with an average of 24%±19. The fact that runoff transmission losses are on average 2.5 times higher during dry field conditions indicates that gully beds are far more efficient in infiltrating surface runoff when dry.

Next to its hydrological condition, the vegetation cover of the gully bed largely affects surface runoff transmission. The formation of vegetated buffer zones in the gully bed adds roughness, retards runoff velocity, disperses flow, and promotes infiltration and deposition of sediment. Plants remove water from the soil, enhancing the capacity to absorb water. Gullies with more than 50% vegetation cover (Carmenjadan1, Jadan1 and Quingeo) have the highest cumulative infiltration coefficients: under dry hydrological conditions, 81% of the total surface runoff infiltrated in the gully bed. This value is reduced to 34% in more moist conditions. Sparsely vegetated gullies, such as Mosquera2 and Sanmiguel2 with vegetation cover below 15%, are characterized by low infiltration coefficients of about 50% under dry conditions, and about 19% under wet conditions.

Infiltration also increased with increasing runoff width. This is to be expected, given the fact that the water can infiltrate over a large area if the runoff width is larger. Linear regression reveals that ca. 78% of the variance in cumulative infiltration coefficient was explained by vegetation cover, runoff width and antecedent moisture content (Tables 2 and 3). Thus, apart from vegetation cover, soil conditions and gully geometry also strongly affect water infiltration into the gully bed.

4 Numerical modeling of runoff transfer in gully channels

4.1 Model calibration

The kinematic wave model was calibrated manually by adjusting the values of sorptivity, S, and hydraulic conductivity, K, in order to match the observed outflow hydrographs (Table 4). Calibration was performed for each flow experiment, and the optimal parameter values for the hydraulic conductivity and sorptivity were chosen based on the closeness of fit of plots of observed and simulated outflow hydrographs (Fig. 4). The model was calibrated for 16 out of 18 flow experiments. The goodness-of-fit between simulated and measured outflow volumes was evaluated based on comparisons of predicted with observed outflow volumes (Table 4 and Fig. 5a), and three statistical measures (Table 5): the root mean square error (RMSE), the coefficient of determination (R^2) and the model efficiency (ME). Figure 5a shows that the model is able to predict the transfer of runoff water generally well, with a slight tendency to underpredict the total outflow volumes. The statistical results obtained with the optimal parameter values show a RMSE of 0.13, a R^2 of 0.91 and a ME of 0.92. These coefficients indicate that the performance of the model was satisfactory and that predictions of outflow volumes were generally good.

One experiment, the San Miguel2 "wet run", shows error on the predicted outflow volume of 23%. This error is mainly related to a poor representation of non-uniform hydrological conditions along the gully bed that existed during the experiment. The poor model prediction for the San Miguel2 gully can be explained by erosion of the gully channel during the dry run. The San Miguel2 gully has steep slopes, and its gully channel is very sparsely vegetated (average vegetation cover of 3%). We observed supercritical flow that eroded rapidly the gully channel during the experiment. As a result, the weathered bedrock was outcropping in several gully segments leading to very low infiltration rates. The presence of patchy rock outcrops in the gully bed, poorly represented in the hydrological model, explains the non-uniform hydrological behaviour of the gully channel.

4.2 Sensitivity analysis

A sensitivity analysis was performed to explore the dependency of the model output on the value of its input parameters. The main factor controlling the hydrology and sedimentology of the gully channel is its vegetation cover (Molina et al., 2009). The effect of vegetation on runoff water transmission is apparent in the parameter values of the Manning's roughness coefficient n, the runoff width W; and the sorptivity S and hydraulic conductivity K of the channel bed. The presence of vegetation cover in the gully bed decelerates runoff flow by increasing the channel bed roughness. Besides, it enhances the porosity and capillarity of the channel bed. In addition to Manning's roughness coefficient, sorptivity and hydraulic conductivity, the runoff width is the most important morphological parameter controlling the effect of vegetation on runoff flow transmission (Fiener and Auerswald, 2005). The sensitivity of the model predictions to variations in the input parameters of the Manning's roughness coefficient n, sorptivity S, hydraulic conductivity K and runoff width W was analysed for the "dry run" Jadan1 experiment. An individual parameter sensitivity analysis was performed by varying one input parameter at a time, starting with the initial values (n=0.252 m s$^{-1/3}$, S=5.156×10^{-4} m s$^{-0.5}$, K=3.918×10^{-5} m s^{-1} and W average=0.77 m). The percentage of change both in total runoff volume and in the prediction of the time to runoff was calculated once the parameter was varied. With variations in the range of model input parameters, the range of computed flow hydrographs at the downstream end of the gully channel was analysed. We chose values of Manning's n of 0.02 m s$^{-1/3}$ for an unvegetated gully bed and 0.3 m s$^{-1/3}$ for a fully vegetated gully bed.

The results of the sensitivity analyses show that the prediction of the time to runoff and the total runoff volume are highly sensitive to the input parameters for S, K and W, and only marginally sensitive to the Manning's n (Fig. 6). A 10% decrease in S translates into a 330% increase in runoff volume and 57% decrease in time to runoff, whereas a 20% decrease in S translates into a 425% increase in runoff volume and 72% decrease in time to runoff (Fig. 6a). An increase in S of only 10% prevents the model to produce any outflow. Similar observations were made for W: a 30% decrease in W translates into a 600% increase in runoff volume and 75% decrease in time to runoff while a 40% decrease in W translates into a 810% increase in runoff volume and 84% decrease in time to runoff (Fig. 6b). Increasing W by 10%, the model is unable to predict any outflow. By changing the parameter value of K by −10%, the computed runoff volume increased by 340% and the time to runoff decreased by 50%, whereas a 20% decrease in K translates into a 515% increase in runoff volume and 65% decrease in time to runoff (Fig. 6c). On the other hand, a 3% increase in K both the runoff volume and the time to runoff were not predicted. The modelled results were marginally sensitivity to changes in Manning's n. Figure 6d shows how a 92% decrease in n (for the unvegetated gully bed scenario, n=0.02 m s$^{-1/3}$) translates into a 35% increase in runoff volume and 11% decrease in time to runoff. Meanwhile a 19% increase in n (for the fully vegetated scenario, 0.3 $\mathrm{m\,s^{-1/3}}$) translates into a 5% decrease in runoff volume and 2% increase in time to runoff.

4.3 Relationship of optimised model parameters with gully characteristics

The analysis above shows that a simple runoff-infiltration model is quite capable of simulating the observed transmission losses, both in terms of total quantities and temporal dynamics. However, application of such a model in conditions where no experimental data are available would require the prediction of the model parameters to which the results are most sensitive with high accuracy, e.g. from observations on vegetation cover in the gully beds.

Correlation analysis shows that the relation between sorptivity, S, and gully characteristics is relatively weak (Table 6). As this might be due to model overparameterization (as both K and S describe the infiltration properties of the gully bed), we carried out a second optimisation procedure whereby we assumed S to be constant and to be equal to the average value ($4.46\times10^{-4}\ \mathrm{m\,s^{-0.5}}$) obtained during the first optimisation and only allowed K to vary. As expected, this resulted in a somewhat lower model performance (Table 4 and Fig. 5b).

Correlation analysis shows that K^* (estimated hydraulic conductivity, after second optimisation) is signficantly related to several gully characteristics (Table 6). These characteristics are often interrelated and therefore we used multiple stepwise regression to assess combined effects, resulting in:

$$K^* = 5.18E^{-5} - (4.93E^{-7} \times \mathrm{ASM}) - (7.56E^{-7} \times \mathrm{Silt}) + (2.97E^{-7} \times \mathrm{VC}) \tag{12}$$

(R^2=0.59, n=16)

The fact that optimised K^* values are dependent on the antedecent soil moisture suggests that either (i) the gully systems did not achieve true steady state during the experiments or (ii) that the model formulation we used does not allow to fully account for transient effects through the sorptivity, S, so that part of these effects are accomodated

HESSD

6, 2537–2571, 2009

Reducing the hydrological connectivity of gully systems

A. Molina et al.

for through variations in hydraulic conductivity K^*. Both factors probably play a role: during some experiments, steady state was clearly not reached and it is therefore likely that our estimate of K^* does not accurately reflect the steady-state value. On the other hand, we represent each gully system using a single hydraulic conductivity value. Given the spatial variation of vegetation cover and sediment thickness within the gully, this is clearly a (necessary) simplification that may result in an estimated K^*-value that is dependent on antecedent moisture content.

K^* is also negatively related to the gully bed's silt content and positively related to vegetation cover. The positive relationship with vegetation cover is as expected: the presence of vegetation and vegetation residue is known to increase the hydraulic conductivity of the topsoil by protecting it against sealing and crusting and by enhancing infiltration through macropores due to roots and/or to the activity of animals living in the vicinity of vegetation. Estimated hydraulic conductivity is negatively related to the gully bed's silt content. Several studies have shown that the presence of silt in a topsoil layer may indeed strongly enhance the reduction of hydraulic conductivity due to sealing and crusting (Poesen, 1986).

While the above analysis shows that our data may be well described using a physically based model, it does not allow us to conclude that a physically based model may be used succesfully for the prediction of runoff transmission losses. We therefore also investigated to what extent predictions of runoff volumes by the model described above agreed with observed values if the hydraulic conductivity predicted by Eq. (12) was used while measured values were used for all other model parameters. Figure 5c shows that predictions are poor. Generally, predicted runoff volumes are of the correct order of magnitude, but the relationship between predicted and observed runoff volumes is not statistically significant. This is not surprising given the high sensitivity of model output to the estimation of hydraulic conductivity: a change of +/−10% in K results in changes in total runoff output of over 300% (Fig. 6c). As the standard errors of predictions using Eq. (12) are well in excess of 30%, an accurate prediction of total runoff volume using predicted values of K cannot be expected. This shows once more that the applicability of physically based models in hydrology is often strongly hampered by our inability to accurately estimate parameter values at the scale required, a problem that has often been discussed in the literature (e.g. Beven, 1995).

Although we may not be able to model the response of each individual gully correctly, our analysis does allow to identify the major controls of water transmission losses on vegetated gully beds. The most important control appears to be the soil moisture status. However, vegetation cover and runoff width also play an important role. The latter two are to some extent interrelated: in a system that is recovering after an intense degradation phase, the re-appearance of vegetation on gully beds will lead to sediment trapping and hence to an increase in runoff width. Any model that aims at reflecting changes in hydrology due to vegetation recovery should therefore incorporate both factors. The model we used may be used to identify trends and estimate the direction and the order of magnitude of change. However, the correct calculation of transmission losses in individual gullies for a given inflow rate using a so-called physically-based model appears not to be possible as the necessary input parameter values cannot be estimated with the required accuracy.

5 Conclusions

Concentrated flow experiments in steep gully channels clearly show that gully systems play a pivotal role in the hydrological response of degraded catchments. They concentrate the surface runoff generated at the hillslopes, and transport it to the river network. Any change in the state of the gully channels largely affects their water transport efficiency. Gullies with more than 50% surface vegetation cover exhibit the highest cumulative infiltration coefficients (81% for “dry runs”, and 34% for “wet runs”). The efficiency of gully bed vegetation in reducing runoff water transfer is the highest for dry gully beds, i.e. at the beginning of a rainfall event.

The experimental field data were used to calibrate a kinematic wave model that predicts the outflow hydrograph at the downstream end of the channel. The effect of vegetation cover on runoff water transmission was incorporated in the hydrological model by parameterizing a vegetation-dependent Manning's roughness coefficient, soil sorptivity and hydraulic conductivity value. The kinematic wave model is able to predict the transfer of runoff water well, as the error on the predicted outflow volumes is below 13% for 15 out of 16 cases. However, its applicability to predict transmission losses for gully systems where no experimental data are available can be questionable, as our results indicate that it remains difficult to accurately predict parameter values at the scale required for these analyses. Correlation analysis between optimised parameter values and gully characteristics indicate that soil moisture content, vegetation cover and runoff width are the major controls of water transmission losses in vegetated gully beds. The interaction of vegetation and runoff width is particularly efficient in retarding surface runoff and enhancing runoff infiltration in dry hydrological conditions. Once the gully bed is wetted, its storage and infiltration capacity are reduced.

The results obtained from the field experiments and the kinematic wave model clearly point to the importance of gully systems in controlling transfer of water and sediment from the slopes towards the river system. Gully systems are key elements in the hydrological connectivity of degraded landscapes, and restoration of gully systems e.g. by vegetation of the channel bed is particularly efficient in reducing water and sediment delivery to the river system.

Acknowledgements. We thank F. Cisneros, M. Ramirez, and E. Tacuri for facilitating equipment utilisation for the field experiments. This work was supported by an IRO fellowship and a PDM postdoctoral mandate from the K. U. Leuven to A. Molina. This research was done within the framework of the Inter-University Project "Towards integrated catchment management in tropical mountain areas: the problem of sediment management, Paute River, Ecuador" between the University of Cuenca, Ecuador and the K. U. Leuven, Belgium.

References

Beven, K.: Linking parameters across scales: Subgrid parameterizations and scale dependent hydrological models, Hydrol. Process., 9, 507–525, 1995.

Bracken, L. J. and Croke, J.: The concept of hydrological connectivity and its contribution to understand runoff-dominated geomorphic systems, Hydrol. Process., 21, 1749–1763, 2007.

Bruijnzeel, L. A.: Hydrological functions of tropical forests: not seeing the soils for the trees?, Agr. Ecosyst. Environ., 104, 185–228, 2004.

Chow, V. T., Maidment, D. R., and Mays, L. W.: Applied Hydrology, McGraw-Hill, USA, 572 pp., 1988.

Cowan, W. L.: Estimating hydraulic roughness coefficients, Agr. Eng., 37, 473–475, 1956.

Croke, J., Mockler, S., Fogarty, P., and Takken I.: Sediment concentration changes in runoff pathways from a forest road network and the resultant spatial pattern of catchment connectivity, Geomorphology, 68, 257–268, 2005.

Deletic, A.: Modelling of water and sediment transport over grassed areas, J. Hydrol., 248, 168–182, 2001.

Dercon, G., Bossuyt, B., De Bièvre, B., Cisneros, F., and Deckers, J.: Zonificación Agroecologica del Austro Ecuatoriano. Programa para el Manejo del Agua y Suelo (PROMAS), Cuenca, Ecuador, 1998.

Fiener, P. and Auerswald, K.: Effectiveness of grassed waterways in reducing runoff and sediment delivery from agricultural watersheds, J. Environ. Qual., 32, 927–936, 2003.

Fiener, P. and Auerswald K.: Measurement and modeling of concentrated runoff in grassed waterways, J. Hydrol., 301, 198–215, 2005.

Harden, C. P.: Andean soil erosion: A comparison of soil erosion conditions in two Andean watersheds, Nat. Geogr. Res. Expl., 7, 216–231, 1991.

Harden, C. P.: Interrelationship between land abandonment and land degradation: a case from the Ecuadorian Andes, Mountain Research and Development, 16, 274–280, 1996.

Harden, C. P.: Human impacts on headwater fluvial systems in the Northern and Central Andes, Geomorphology, 79, 249–263, 2006.

Hillel, D.: Environmental Soil Physics, Academic Press, San Diego, CA, 1998.

Hungerbühler, D., Steinmann, M., Winkler, W., Seward, D., Eguez, D., Eguez, A., Peterson, D. E., Helg, U., and Hammer, C.: Neogene stratigraphy and Andean geodynamics of southern Ecuador, Earth Sci. Rev., 57, 75–124, 2002.

Janeau, J. L., Bricquet, J. P., Planchon, O., and Valentin, C.: Soil crusting and infiltration on steep slopes in northern Thailand, Euro. J. Soil Sci., 54, 543–553, 2003.
Le Bissonnais, Y., Lecomte, V., and Cerdan, O.: Grass strip effects on runoff and soil loss, Agronomie, 24, 129–136, 2004.
Lighthill, M. J. and Woolhiser, D. A.: Modern approach to design of grassed channels, J. Irrigat. Drain. Eng. ASCE, 118, 733–743, 1955.
Lopez, F. and Garcia, M. H.: Mean flow and turbulent structure of open-channel flow through non-emergent vegetation, J. Hyd. Eng., 127, 392–402, 2001.
Molina, A., Govers, G., Vanacker, V., Poesen, J., Zeelmaekers, E., and Cisneros, F.: Runoff generation in a degraded Andean ecosystem: Interaction of vegetation cover and land use, Catena, 71, 357–370, 2007.
Molina, A., Govers, G., Cisneros, F., and Vanacker, V.: Vegetation and topographic controls on sediment deposition and storage on gully beds in a degraded mountain area, Earth Surface Processes and Landforms, doi:10.1002/esp.1747, in press, 2009.
Muñoz-Carpena, R., Miller, C. T., and Parsons, J. E.: A quadratic Petrov-Galerkin solutions for kinematic wave overland flow, Water Resou. Res., 29, 2615–2627, 1993.
Muñoz-Carpena, R., Parsons, J. E., and Gilliam, J. W.: Modeling hydrology and sediment transport in vegetative filter strips, J. Hydrol., 214, 111–129, 1999.
Nachtergaele, J., Poesen, J., Wijdenes, D. O., and Vandekerckhove, L.: Medium-term evolution of a gully developed in a loess-derived soil, Geomorphology, 46(3–4), 223–239, 2002.
Philip, J. R.: Theory of infiltration, Adv. Hydrosci., 5, 215–296, 1969.
Poesen, J.: Surface sealing as influenced by slope angle and position of simulated stones in the top layer of loose sediments, Earth Surf. Processes, 11, 1–10, 1986.
Prosser, I., Dietrich, W., and Stevenson, J.: Flow resistance and sediment transport by concentrated overland flow in a grassland valley, Geomorphology, 13, 71–86, 1995.
Rey, F.: Influence of vegetation distribution on sediment yield in forested marly gullies, Catena, 50, 549–562, 2003.
Rey, F.: Effectiveness of vegetation barriers for marly sediment trapping, Earth Surf. Processes, 29, 1161–1169, 2004.
Seibert, J. and McGlynn, B.: Landscape element contributions to storm runoff, In Encyclopedia of Hydrological Sciences, edited by: Anderson, M. G., Wiley: Chichester, UK, 1751–1761, 2005.
Temple, D. M.: Flow retardance of submerged grass channel linings, Transactions of the Amer-

ican Society of Agricultural Engineers, 25, 1300–1303, 1982.
Temple, D. M.: Design of grass-lined open channels, Transactions of the American Society of Agricultural Engineers, 26, 1064–1069, 1983.
Tsujimoto, T.: Fluvial processes in streams with vegetation, J. Hyd. Res., 37, 789–803, 1999.
Vanacker, V., Govers, G., Barros, S., Poesen, J., and Deckers, J.: The effect of short-term socio-economic and demographic changes on land-use dynamics and its corresponding geomorphic response with relation to water erosion in a tropical mountainous catchment, Ecuador, Landscape Ecology, 18, 1–15, 2003.
Vanacker, V., von Blanckenburg, F., Govers, G., Molina, A., Poesen, J., Deckers, J., and Kubik, P.: Restoring natural vegetation reverts mountain erosion to natural levels, Geology, 35, 303–306, 2007.
White, S. and Maldonado, F.: The use and conservation of national resources in the Andes of southern Ecuador, Mountain Research and Development, 11, 37–55, 1991.
Woolhiser, D. A.: Simulation of unsteady overland flow, in: Unsteady flow in open channels, Vol. 2, edited by: Mahmood, K. and Yevjevich, V., Fort Collins, Water Resources, 1975.
Ziegler, A. D., Giambelluca, T. W., Plondke, D., Leisz, S., Tran, L. T., Fox, J,. Nullet, M. A., Vogler, J. B., Troung, D. M., and Vien, T. D.: Hydrological consequences of landscape fragmentation in mountainous northern Vietnam: Buffering of Hortonian overland flow, J. Hydrol., 337, 52–67, 2007.

Table 1. Input parameters of the flow model.

Characteristics	Parameter	Symbol	Unit	Range
Soil	Hydraulic conductivity	K	$m\,s^{-1}$	1.0×10^{-8}–4.8×10^{-5}
	Sorptivity	S	$m\,s^{-0.5}$	9.0×10^{-6}–1.05×10^{-3}
Vegetation	Manning's roughness coefficient	n	$s\,m^{-1/3}$	9.1×10^{-2}–2.52×10^{-1}
Hydrology component	Hydraulic radius	R	m	0.032–0.15
	Average runoff width	W	m	0.51–1.09
	Average flow depth	y	m	0.035–0.37
	Distance in flow direction	x	m	5
	Average flow velocity	v	$m\,s^{-1}$	0.261–1.394
	Average bed slope	So	$m\,m^{-1}$	0.14–0.56
	Inflow	Q	$m^3\,s^{-1}$	0.0019–0.0027
	alpha	α	dimensionless	0.238–0.9187
	beta	β	dimensionless	0.6

HESSD

6, 2537–2571, 2009

Title Page
Abstract | Introduction
Conclusions | References
Tables | Figures
Back | Close
Full Screen / Esc
Printer-friendly Version
Interactive Discussion

HESSD

6, 2537–2571, 2009

Reducing the hydrological connectivity of gully systems

A. Molina et al.

Table 2. Summary of the experimental data of the concentrated flow experiments (Note that the dry run experiments are marked by an asterisk).

Location	Total inflow volume RI m^3	Total outflow volume RO m^3	Total infiltration volume I m^3	Cumulative infiltration coefficient IC %	Average vegetation cover VC %	Antecedent soil moisture ASM %	Average bed slope *So* %	Average runoff width *W* m	Sand %	Silt %	Clay %
Carmenjadan1*	2.77	1.44	1.33	48	70	49	23	0.81	43	48	9
Carmenjadan1	2.14	2.11	0.03	1	70	56	23	0.81	43	48	9
Carmenjadan2*	3.37	2.00	1.37	41	24	30	18	0.51	29	56	15
Carmenjadan2	1.90	1.49	0.41	22	24	55	18	0.51	29	56	15
Jadan1*	3.79	0.19	3.59	95	77	10	56	0.77	45	40	15
Jadan1	2.20	0.67	1.54	70	77	14	56	0.77	45	40	15
Jadan2*	2.57	1.69	0.88	34	43	6	55	1.09	32	53	15
Jadan2	2.06	1.84	0.22	11	43	16	55	1.09	32	53	15
Mosquera1*	2.80	1.40	1.40	50	35	12	40	0.66	14	52	34
Mosquera1	2.02	1.61	0.41	20	35	29	40	0.66	14	52	34
Mosquera2*	3.04	1.15	1.89	62	12	11	27	0.55	55	36	9
Mosquera2	1.99	1.60	0.39	20	12	38	27	0.55	55	36	9
Sanmiguel1*	3.84	1.63	2.21	58	34	14	27	0.62	4	55	41
Sanmiguel1	1.92	1.51	0.41	21	34	34	27	0.62	4	55	41
Sanmiguel2*	3.47	1.65	1.82	52	3	15	34	0.60	47	38	15
Sanmiguel2	1.67	1.38	0.29	17	3	29	34	0.60	47	38	15
Quingeo*	5.99	0.00	5.99	100	59	–	14	–	–	–	–
Quingeo	5.22	3.54	1.68	32	59	–	14	–	–	–	–

HESSD

6, 2537–2571, 2009

Table 3. Results of the multiple regression analysis for the prediction of the cumulative infiltration coefficient, IC. The uncertainty on the model fit is given by the partial and model R-Square.

		Parameter estimate	p-value	Partial R-Square	Model R-Square
Antecedent soil moisture	ASM	−1.270	<0.001	0.348	0.348
Average vegetation cover	VC	0.754	0.0007	0.109	0.457
Runoff width	*W*	−102.049	0.0011	0.326	0.784

Table 4. Results of the kinematic flow model for each gully system with indication of the calibrated and predicted parameter values and the predicted outflow (Note that the dry run experiments are marked by an asterisk). K^* and predicted outflow* were obtained after a second model optimisation keeping the sorptivity, S, constant. The values of predicted outflow(*) were obtained using the predicted values of K^* after Eq. (12).

Location	n s m$^{-1/3}$	S m s$^{-0.5}$	K m s^{-1}	Measured outflow m^3	Predicted outflow m^3	Error %	K^* m s^{-1}	Predicted Outflow* m^3	Predicted Outflow(*) m^3
Carmenjadan1*	0.231	5.07×10^{-4}	1.0×10^{-6}	1.44	1.31	−9	9.70×10^{-6}	1.09	0.58
Carmenjadan1	0.212	1.2×10^{-4}	2.0×10^{-7}	2.11	2.18	3	1.0×10^{-6}	1.49	1.06
Carmenjadan2*	0.169	1.05×10^{-3}	1.14×10^{-6}	2.00	1.83	−9	1.0×10^{-5}	2.71	2.98
Carmenjadan2	0.160	7.2×10^{-4}	5.0×10^{-7}	1.49	1.42	−5	1.0×10^{-5}	1.46	1.62
Jadan1*	0.252	5.156×10^{-4}	3.918×10^{-5}	0.19	0.20	4	4.58×10^{-5}	0.14	0.91
Jadan1	0.230	3.8×10^{-4}	4.8×10^{-5}	0.67	0.68	1	4.70×10^{-5}	0.63	0.86
Jadan2*	0.230	5.965×10^{-4}	6.388×10^{-7}	1.69	1.56	−8	2.35×10^{-5}	0.80	0.63
Jadan2	0.214	9.0×10^{-6}	7.0×10^{-6}	1.84	1.74	−6	9.0×10^{-7}	1.21	0.37
Mosquera1*	0.195	7.15×10^{-4}	9.9×10^{-7}	1.40	1.45	4	1.0×10^{-6}	2.18	1.42
Mosquera1	0.182	3.0×10^{-4}	9.9×10^{-8}	1.61	1.70	5	1.0×10^{-6}	1.44	1.15
Mosquera2*	0.157	4.2×10^{-4}	3.7×10^{-5}	1.15	1.10	−4	3.60×10^{-5}	1.10	1.62
Mosquera2	0.155	1.95×10^{-4}	9.0×10^{-6}	1.60	1.63	2	1.0×10^{-6}	1.60	1.38
Sanmiguel1*	0.185	6.2×10^{-4}	1.9×10^{-5}	1.63	1.72	6	2.20×10^{-5}	1.98	2.44
Sanmiguel1	0.177	9.0×10^{-5}	8.0×10^{-6}	1.51	1.63	8	1.0×10^{-6}	1.44	1.36
Sanmiguel2*	0.106	5.35×10^{-4}	9.2×10^{-6}	1.65	1.43	−13	1.67×10^{-5}	1.21	1.23
Sanmiguel2	0.104	4.0×10^{-4}	5.0×10^{-6}	1.38	1.06	−23	2.0×10^{-6}	1.09	0.83

HESSD

6, 2537–2571, 2009

HESSD

6, 2537–2571, 2009

Reducing the hydrological connectivity of gully systems

A. Molina et al.

Table 5. Statistics used to assess the goodness of the model.

Description	Symbol	Equation	Best fit
Root Mean Square Error	RMSE	$\mathrm{RMSE} = \sqrt{\frac{1}{n}\sum_{i=1}^{n}(O_i - P_i)^2}$	0.0
Coefficient of Determination	R^2	$R^2 = 1 - \frac{\frac{1}{(n-2)}\sum_{i=1}^{n}(O_i - P_i)^2}{\frac{1}{(n-1)}\sum_{i=1}^{n}(O_i - O_{i\,\mathrm{mean}})^2}$	1.0
Model Efficiency	ME	$\mathrm{ME} = 1 - \frac{\sum_{i=1}^{n}(O_i - P_i)^2}{\sum_{i=1}^{n}(O_i - O_{i\,\mathrm{mean}})^2}$	1.0

Table 6. Pearson correlation coefficients (n=16) between K, S and K^*, and the gully characteristics. K^* is obtained after a second model optimisation keeping the value of sorptivity, S, constant. (Note that the values in italics represent the p-values).

		Hydraulic Conductivity K	Sorptivity S	Hydraulic Conductivity K^*
Runoff width	W	−0.043	−0.354	0.085
		0.873	*0.177*	*0.753*
Average vegetation cover	VC	0.303	−0.157	0.371
		0.253	*0.560*	*0.156*
Cumulative Infiltration coefficient	IC	0.746	0.438	0.848
		0.0009	*0.0893*	*<0.0001*
Antecedent soil moisture	ASM	−0.505	−0.147	−0.544
		0.045	*0.586*	*0.029*
Average bed slope	So	0.425	−0.217	0.457
		0.100	*0.419*	*0.075*
Sand	–	0.334	−0.122	0.326
		0.205	*0.650*	*0.216*
Silt	–	−0.546	0.243	−0.394
		0.028	*0.364*	*0.130*
Clay	–	−0.121	0.015	−0.213
		0.653	*0.955*	*0.426*

Fig. 1. Experimental design of the concentrated flow experiments with **(a)** water supply from water tank, **(b)** and **(c)** concentrated flow in the gully floor, and **(d)** collection of runoff water and sediment.

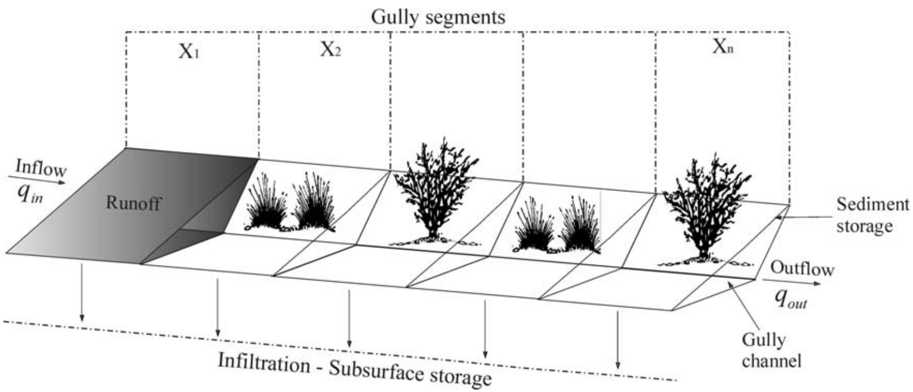

Fig. 2. Schematic illustration of model components.

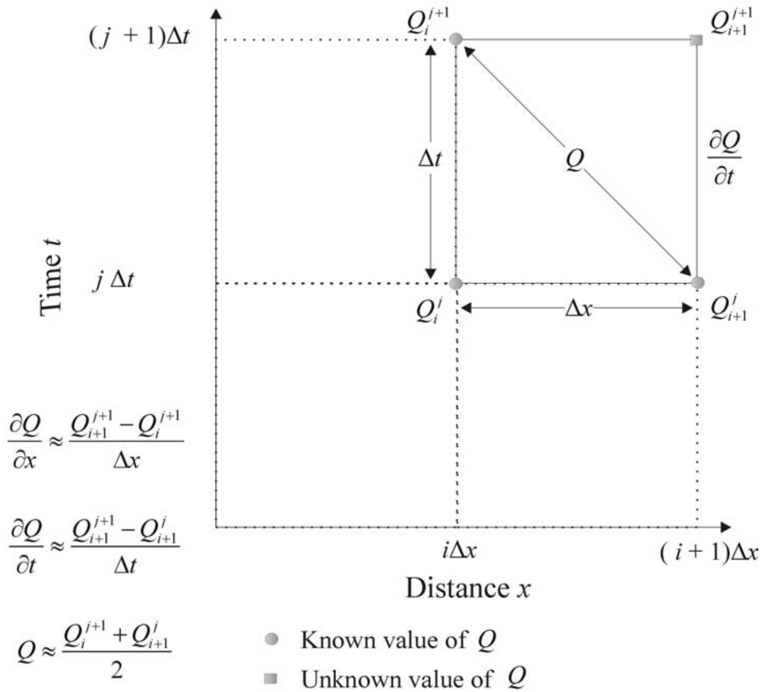

Fig. 3. Outline of the computational grid used to solve the kinematic wave equation (after Chow et al., 1988).

HESSD
6, 2537–2571, 2009

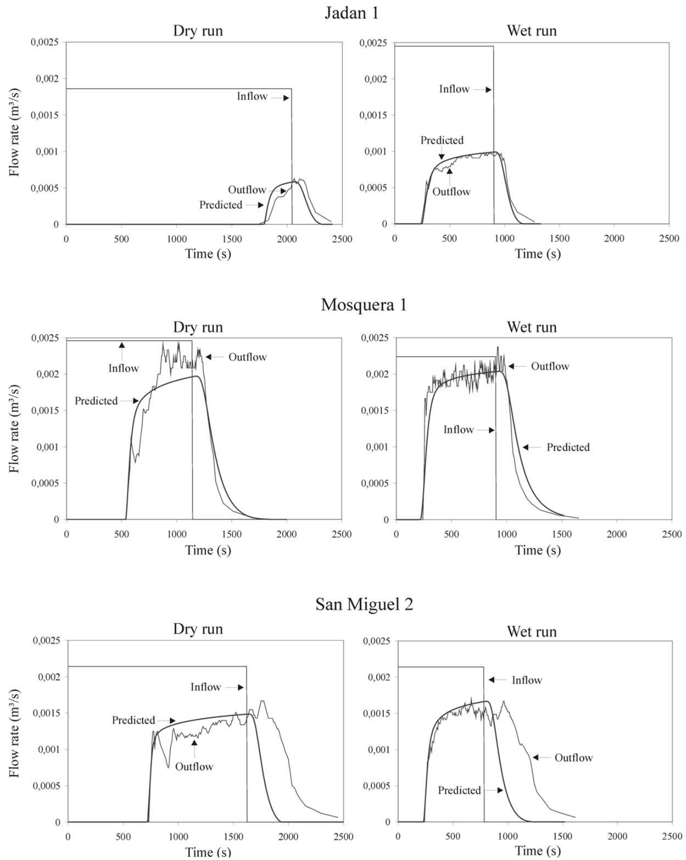

Fig. 4. Observed and computed flow hydrograph for three gullies with distinct vegetation cover of the gully bed (Jadan1: dense vegetation cover, Mosquera1: intermediate vegetation cover, and San Miguel2: very low vegetation cover of gully bed).

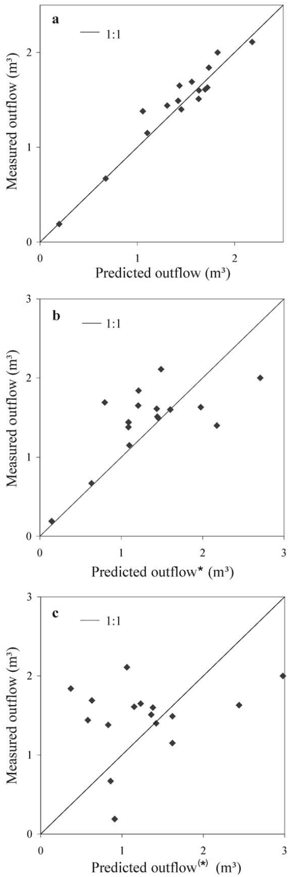

Fig. 5. Plots of measured vs. predicted outflow volume for the 16 runs. **(a)** Predicted outflow is obtained by calibrating K and S to match the observed outflow hydrograph, **(b)** Predicted outflow (outflow*, second optimisation) is predicted by keeping the sorptivity, S, constant and equal to the average S-value obtained from the first optimisation, and **(c)** Predicted outflow, outflow(*), is calculated using the predicted values of K^* from the regression Eq. (12).

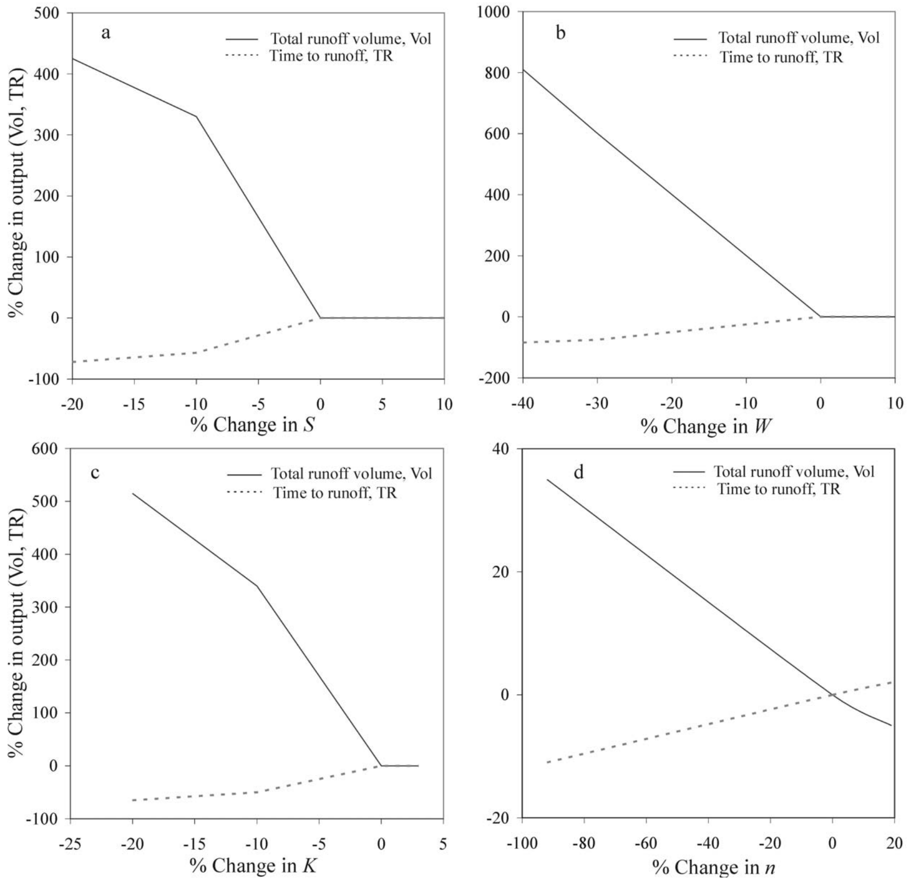

Fig. 6. Sensitivity of the model to changes in the input values of the sorptivity, runoff width, hydraulic conductivity and Manning's roughness coefficient.